Conference Presentation

Use of a NOM profilometer to measure large aspheric surfaces

Pearson, J.L., Roberts, G.W., Rees, P.C.T. and Thompson, S.J.

This is a paper presented at the Optical Fabrication, Testing, and Metrology V conference, 7-10 September 2015, Friedrich-Schiller-University, Jena, Germany

The definitive version of this paper is published by SPIE and is available at:
http://proceedings.spiedigitallibrary.org/proceeding.aspx?articleid=2443977

Use of a NOM profilometer to measure large aspheric surfaces

Gareth W. Roberts*[a], John L. Pearson[a], Paul C.T. Rees[a], Samantha J. Thompson[b]

[a]Glyndŵr University, OpTIC Glyndŵr, Ffordd William Morgan, St. Asaph, Denbighshire, LL17 0JD, UK; [b]Cavendish laboratory, University of Cambridge, Cambridge, CB3 0HE, UK.

ABSTRACT

The use of autocollimator-based profilometers of the Nanometer Optical measuring Machine (NOM) design has been reported for the evaluation of X-ray optics for some time. We report a related development in the use of a non-contact NOM profilometer for the *in situ* measurement of base radius of curvature and conic constant for E-ELT primary mirror segments during fabrication. The instrument is unusual in NOM design in that it is deployable onto a CNC polishing machine in an industrial fabrication environment. Whilst the measurement of radius of curvature of spherical surfaces over a single scan has been reported previously, here we report on the use of this instrument to measure optical surfaces with an aspheric departure of 180 micrometers using a grid of multiple scans and bespoke surface fitting software. The repeatability of the measurement has been found to be approximately 1 mm in a measured radius of curvature of approximately 90 m. The absolute accuracy is limited by the accuracy of the calibration of the autocollimator and the *in situ* calibration of the instrument during operation.

Keywords: nanometer optical measuring machine, NOM, non-contact, profilometry, on-machine metrology, aspheric surfaces

1. INTRODUCTION

Many ground- and space-based reflecting telescopes are now adopting a segmented design for their primary reflecting mirror in order to increase their light- and information-gathering capacity. The European Southern Observatory (ESO) plans to build a ground-based facility, the "European Extremely Large Telescope" (E-ELT), which is intended to be the world's largest ground-based reflecting telescope when built by 2024.

The current specification for the E-ELT main primary mirror (M1) requires a total of 798 hexagonal-shaped segments, resulting in a primary mirror diameter of 39 m and a base radius of curvature of 69 m. In 2007 ESO tendered for the test production of several prototype hexagonal-shaped, segments, each 1.4m at full aperture and with an aspheric surface. Glyndŵr University and partners secured a contract to produce the segments which were to be polished to within specification from mainly hexagonal-shaped aspherized blanks.

In order to allow *in situ* interferometry measurements of segments at various stages of the polishing campaigns, Glyndŵr University built an optical test tower around a CNC polishing machine. Reference spherical surfaces could also be measured *in-situ*, in a "piggy-back" manner above the segment. As interferometry cannot directly measure a radius of curvature, an additional, independent method had to be developed and incorporated when required, with the same level of *in situ* convenience.

This paper describes such an experimental configuration, developed at Glyndŵr University, which adopts a non-contact profilometric strategy for measuring aspheric surfaces. In particular, we address:

1. the types of aspheric surfaces derived from the specification;
2. the strategy used to measure them and how it differs from measuring spherical surfaces;
3. how this approach was implemented using the Glyndŵr University NOM, including an error analysis;
4. how the data resulting from measurements was processed and analyzed;
5. a review of the results and their uncertainty and repeatability, with specific examples.

2. THE SURFACES TO BE MEASURED

At the time of adoption in 2007 the ESO design for M1 required that the surface be ellipsoidal with nominal base radius of curvature (R_B) of 84 m and conic constant (k) of -0.993295. The detailed specification included the following points.

*email: g.w.roberts@glyndwr.ac.uk

1. The physical dimensions of the hexagonal segments, in particular the corner-to-corner length of 1.4 m, the position of each segment center vertex relative to the global M1 x-y coordinate system and the substrate materials to be used.
2. The first polished segment should satisfy $R_B = (84.0 \pm 0.2)$ m and R_B for all segments should be known to an accuracy better or equal to 14 mm.
3. The maximum allowable misfigure over the useful area of any polished segment should be 7.5 nm RMS.

3. THE GLYNDŴR NOM

The NOM developed at Glyndŵr University is based on a similar device used at the Diamond Light Source[1] synchrotron facility which in turn was based on a design at BESSY[2,3]. The former organization also assisted with the R&D along with support from the Science Technology Facilities Council (STFC) at Daresbury, U.K. Stringent temperature and vibration control installed for synchrotron purposes enables measurements from these devices with accuracy down to sub-nanometer levels. It was proposed that such a device could be developed for resolving surfaces with a change in curvature or sagitta of the order of ≤ 70 nm RMS, provided temperature is controlled to within $\pm$ 1°C. A change in R_B of 14 mm, see Section 2, corresponds to a change in segment surface sagitta of about 430 nm. In order to ensure measurement accuracy, a repeatability target of about 50 nm RMS or less was chosen at the design stage. This constraint reduces uncertainty in radius to about 2 mm.

The stringent accuracy requirements and strong preference for a non-contact method precluded the use of CMM and laser tracking technology and a long trace profiler system was discounted because of perceived alignment and calibration issues in a production environment. An autocollimator-based NOM system is a non-contact method and proven to be very accurate for small incident angles under closely controlled laboratory environments, although a disadvantage is the restricted angle measurement range. Such a system was selected and the design challenge was to adapt the NOM technique to a less well controlled environment and meet the measurement range and accuracy specification.

The set of design goals for the Glyndŵr NOM included the following:

1. It should measure 1.4 m wide, aspheric surfaces with a nominal base radius of curvature of 84 m and an aspheric departure of 180 micrometers.
2. It should measure unambiguously surface sagitta departures of about 430 nm, which correspond to a radius departure of 14 mm on the scale specified above and to measure with sufficient repeatability, it should be capable of measuring surface sagitta departures of about 50 nm, which correspond to a radius departure of 2 mm.
3. It should be portable and allow rapid deployment in an industrial fabrication environment.

The general configuration is shown schematically in Figure 1, with photographic representations shown in Figure 2 which also shows the local NOM coordinate system (X, Y, Z) and the C-axis. To allow measuring in different scan directions, the rotational C-axis of the CNC polishing machine is used to rotate the segments and their supports rather than rotating the NOM device. The NOM is supported on the moveable bridge of the CNC polishing machine which allows accurate positioning for the individual scanlines. Translation along a scanline in the X direction is achieved by moveable components on the NOM.

Surface slopes are acquired periodically, or discretely, along a scanline using a Möller-Wedel® Elcomat™ 3000 autocollimator whose beam is deflected to the surface by a travelling pentaprism mounted on an air-bearing carriage surrounding a granite beam support. The pentaprism carriage is driven along the granite beam by a stepper motor rack and pinion combination where the aluminum rack runs alongside the granite beam. An incremental encoder tape is fixed to the rack and read by a detector attached to the carriage. This tape can be subject to errors arising from temperature-induced expansion and changes to the support tension of the track and care has to be taken to calibrate the tape whenever this tension is adjusted.

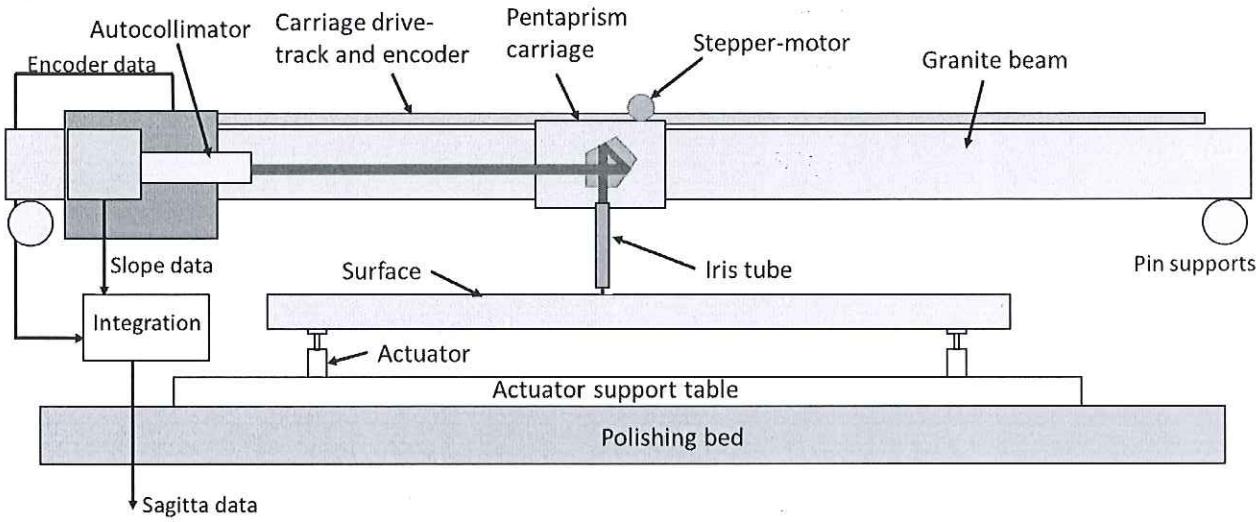

Figure 1. A schematic of the operational principle of the NOM as developed at Glyndŵr University. The slope of the surface being measured is acquired by an autocollimator/pentaprism/iris tube assembly, with the pentaprism being translated along a granite beam by an air-bearing carriage driven by a stepper motor. A metal V-block locates the granite beam to the left support pin, while a curved "rocker" surface rests on the other, see also Figure 2. The slope data, along with its relative position determined by encoder tape, is integrated over position to obtain an array of sagittal values.

Slopes are integrated with respect to the relative position as measured by the encoder tape, which gives an array of the sagittal or Z-component values of the scanline. The pentaprism ensures the net angle of deflection remains constant at a nominal 90 degrees regardless of pitching of the component in operation - there is a significant gravitational sagitta of about 50 microns in the granite beam in response to its own weight and that of the moving carriage. The autocollimator detects surface slope angles about the two local orthogonal axes X and Y which are output and stored by the NOM control software for subsequent post-processing. Polished glass surfaces have about a 4% reflectivity and there is a compromise between allowing enough light to strike the surface, but not with an excessive beam diameter such that the slope detected is ambiguous - the iris tube controls this.

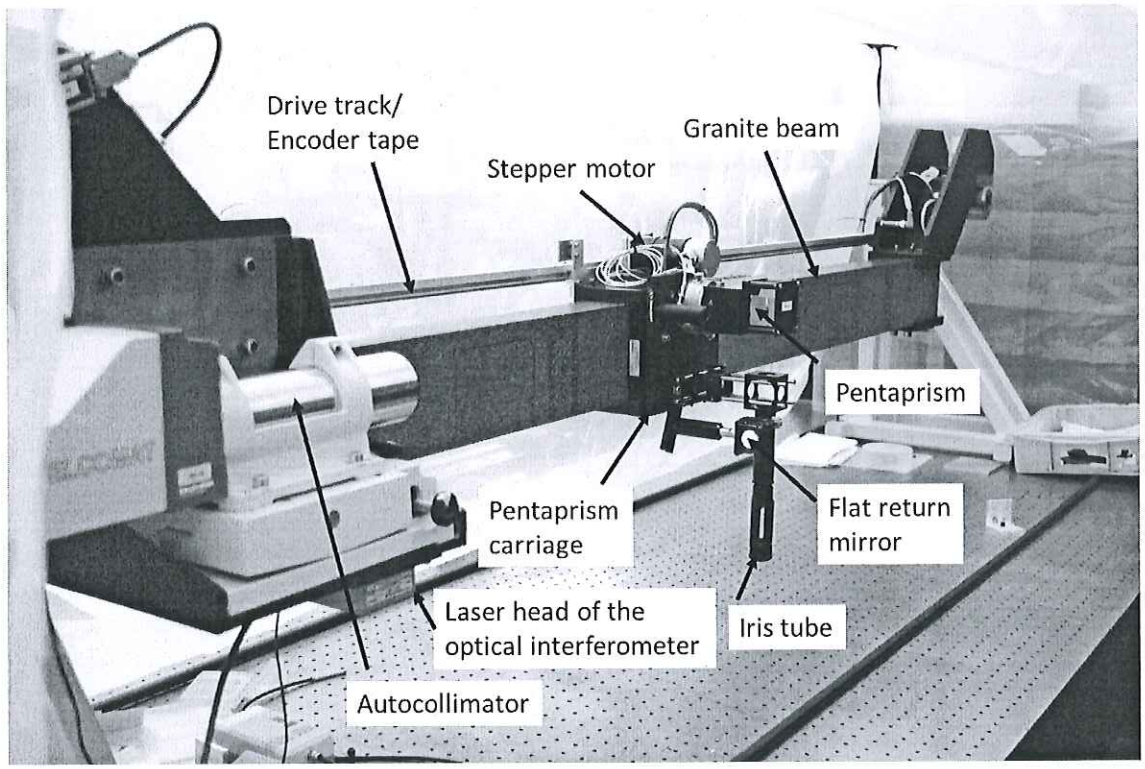

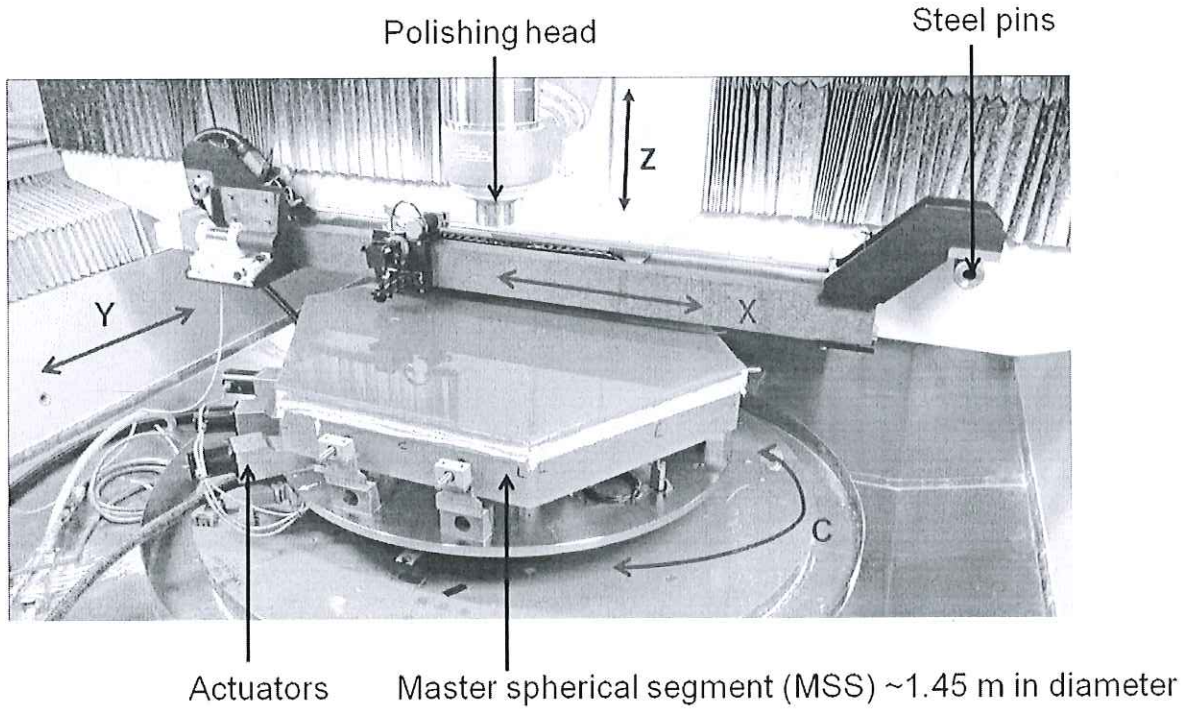

Figure 2. The NOM configurations generally deployed. Upper: the bench configuration illustrating the main components. Also shown is the laser interferometer and return mirror used for an independent optical assessment or calibration of the output displacement of the encoder tape. Lower: the *in situ* configuration on the Zeeko® CNC polishing machine above the surface being polished/measured. The optic being measured in the photo is the 1.45 m master spherical segment (MSS) used for interferometry reference which has a nominal radius of curvature of 84m. The NOM is supported on the moveable bridge of the CNC polishing machine.

The autocollimator has to perform to specification over a wide scan range from about 0.5 m to 2.15 m and thus care has to be taken that possible deviations from factory calibration and/or published specification are accounted for. For that range, the encoder outputs corresponding displacements between 0 m and 1.65m and the practical limit of the range as read by the encoder is about 1540 mm which is sufficient to span the required aperture of the segments.

To cover the whole aperture of the segments with a nominal R_B of 84m, an autocollimator with a ± 1500 arcsec slope range is required. Generally available autocollimators are limited to smaller calibrated ranges, therefore a segment tilting scheme was developed to extend the measurement aperture. A given scan-line was divided into two separate overlapping scans, separated by a segment tilt using the actuators, see Figure 1, then the data "stitched" together in post-processing. However, repeatability and consistency proved difficult to maintain with this approach because of physical segment distortion and the increased degrees of freedom caused issues with data convergence during post-processing.

Extending the specified range from ± 1000 arcsec to ± 1500 arcsec in both the X and Y detection ranges of the autocollimator has little effect on the accuracy and precision of the data and the derived fits to the surface. Based on these findings it was decided to adopt scans without any intermediate tilting, provided care was taken to level the segments prior to measurement so that scans approximately bisected a zero slope. Factory calibration of the autocollimator is accomplished at a single operational distance of 90 mm, therefore it is important to assess the effect of slope-angle deviation on the variable distance range encountered in this configuration. This is discussed further in Section 5.1.

4. MEASUREMENT STRATEGY

The surface form of a conic is given by Equation 1

$$z(x,y) = \frac{\frac{1}{R_B}(x^2+y^2)}{1+\sqrt{1-(1+k)\left(\frac{1}{R_B}\right)^2(x^2+y^2)}}, \quad (1)$$

where $z(x,y)$ is the two-dimensional sagittal field of M1 corresponding to the $x-y$ plane, R_B is the base radius of curvature and k is the conic constant representative of the radial asphericity.

Considering the requirements listed in Section 2, the configuration developed must have the capability to:

1. scan up to 1.4 meters;
2. cover sufficient area of the surface to be representative and in a manner that maintains accuracy and precision within specification;
3. measure the segment in two orthogonal directions: firstly, the direction parallel to the radial lines of M1 over which the asphericity has a maximum component; secondly, the direction perpendicular to the radial lines, i.e. tangential to the azimuthal lines of M1. Over a given measurement path location or scanline, the first will output local radii of curvature which will change value along the scan, while the latter will output nominally constant local radii of curvature along the scan.

Based on the three points above, a plausible measurement campaign to determine R_B and k has two sets of parallel scanlines across the extent of the segment.

Scans will produce an array of sagittal values, Z, with respect to the local coordinate system of the measuring device. These can be referred by translation to a local set of coordinates defined by the geometry of the segment being measured. Knowing the location of the segment center vertex in the global x – y plane of M1 will then allow a base radius and conic constant to be derived using a nonlinear least squares fit to the conic surface of Equation 1. Reference to Figure 3 will show that most segments have scanline sets which are not parallel or perpendicular to their straight edges in order to satisfy point 3 above.

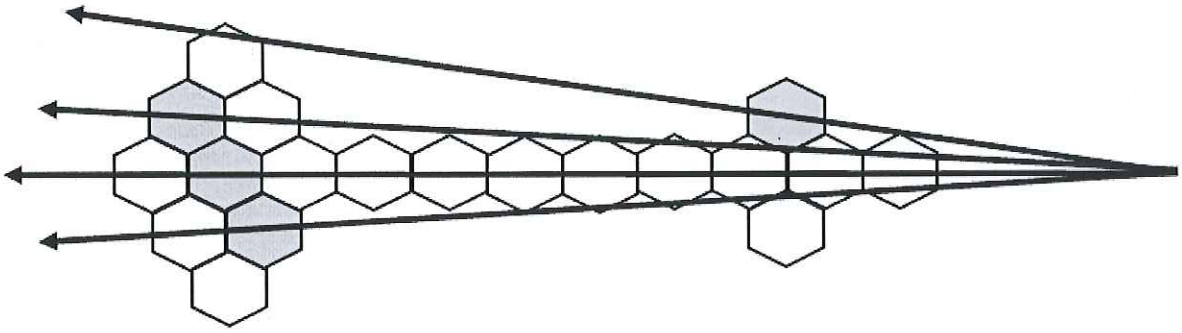

Figure 3. Schematic showing how the directions of four radial lines, emanating from an assumed center vertex of a primary mirror, pass through a section of contiguous segments. Four segments are highlighted as the lines pass through their geometric centers. In this way, it can be envisaged that most segments will have scanlines not parallel or normal to the edges.

An example set of measurement scanlines is shown in Figure 4. In this specific case, the scanlines are equally spaced and parallel or perpendicular to the azimuthal segment edges.

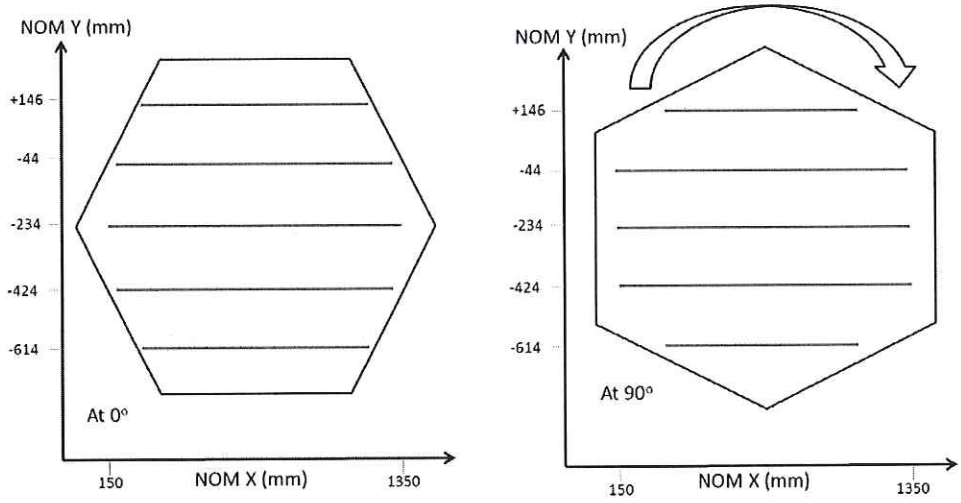

Figure 4. A possible scanline array deployed based on hexagonal segments. Scanlines are equally spaced in the Y coordinate system of the measuring device (NOM). Scans proceed along the X-direction as defined in the coordinate system of the NOM. Note the relative 90 degree rotation required between the two configurations shown in order to measure along both orthogonal directions. These two sets comprise the minimum to determine a base radius and conic constant.

Although the two orientations shown constitute the minimum amount of data required for a surface fit, in practice another two are measured at 180 and 270 degrees. The data from two orientations constitute a "dataset" and two datasets are usually acquired in a measurement campaign. The number of scanlines and scan times must be chosen to optimize the time taken for measurement but without compromising the required accuracy and precision.

Spherical surfaces can be measured in a similar way. For hexagonal-edged examples, scanlines directed corner-to-corner are an obvious option, but many other patterns are possible. Results for the nominal 84m reference spherical surface, deployed during interferometry campaigns, have been reported previously[4].

5. ERROR ANALYSIS

The NOM system serves as an independent check of the base radius of curvature, R_B, and the conic constant, k, and it is essential to know how accurately these parameters can be measured in order to support or validate the interferometric data. The errors inherent in the NOM measurement system must be estimated to ensure that it can measure reliably and consistently to within the tolerance of ESO specification.

The measurement specification requires that the R_B of each segment should be known to accuracy better or equal to 14 mm with the implication that the measurement uncertainty should be kept below about a fifth of that value, i.e. ± 3 mm. The paper by Atkins *et al*[4] presents an error analysis which investigates the effects of environmental temperature and scan time resulting in an estimated measurement error of about 2.5 mm in the radius of spherical surfaces with a nominal radius of 84m.

In this paper we will describe a simple approach to determine an additional absolute error of the system which is dependent on the installed equipment and typical scan lengths deployed. This value is then combined with the typical measurement scatter found when measuring actual segments and reference spheres, similar to the values derived as reported previously in Atkins *et al*[4]. The measurement uncertainty described in this paper will be examined primarily through repeatability tests conducted on the segments. Since the work described in Atkins *et al*[4], temperature control has significantly improved (± 0.25°C) with better air circulation which has reduced shorter-term and longer-term noise in both interferometry and profilometry.

5.1 Encoder tape and autocollimator calibration

Calibration of the encoder tape is necessary when its mount, the aluminum motor-drive-track, requires re-tensioning as that could stretch or contract the tape. For this, an independent SIOS® laser displacement interferometer is deployed, see upper picture in Figure 2. From the difference between the displacement outputs of the laser-interferometer and the encoder tape, a calibration curve is produced and a maximum error determined (about 8 microns in Figure 5 as an example). This is much greater than the specified resolution (0.5 micron) of the tape and it is also temperature-dependent. In this case the encoder output slightly overestimated displacement by an average of 4.7 microns relative to the independent optical method whose uncertainty was estimated at about 70nm over a 1.5m range. For reference, the largest difference measured has been a 70 micron overestimate and a 1°C change in temperature causes about a 10% difference.

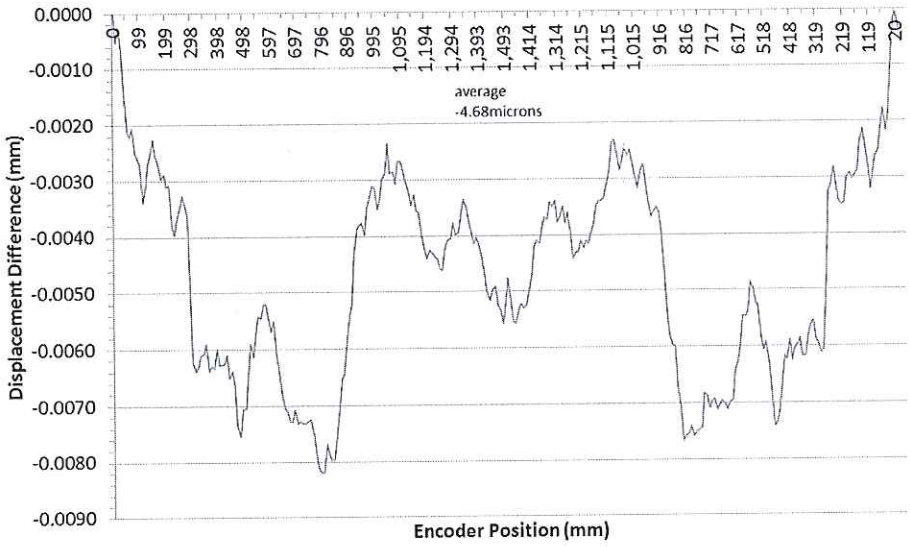

Figure 5. The difference in output displacement between an optical interferometer and the encoder tape system currently installed. Measurement covered one forward and one backward scan consecutively.

The autocollimator is factory calibrated at a single operating distance of 90 mm and over an angle range of ± 1000 arcsec. A range of ± 1500 arcsec would be preferable in order to cover adequately the segments having a base radius of curvature of 84 m,. In addition, the autocollimator-to-surface distance varies considerably from about 0.5 m to 2.15 m during acquisition. A Taylor-Hobson® TA48 small angle generator is currently being used to test the effect of varying operating distance and extending the slope-angle range. Initial results conducted on the bench show that the slope-angle response of the autocollimator to set input angles is not flat. Generally, there is non-zero deviation (measured angle minus set angle), which increases with operating distance. The maximum deviations found were always below 1 arcsec.

At the time of writing, more testing and analysis is required and any compensation is not included in the results shown here.

5.2 Other design-induced errors

For portability, the Glyndŵr NOM has an integrated design and its structure deforms slightly as the carriage transits the granite beam. The most significant of these is a small pitching of the autocollimator and associated beam relative to the bed of the polishing machine or other location which supports the surface being measured. This pitching is only about 2 arcsec over a scan length of about 1530 mm, but is non-symmetrical and is sufficient to change the typical radius of curvature found here by about 25mm.

To compensate for the autocollimator deflection, two measurements are carried out *in situ* before and after the surface measurements, i.e. the surface measurements are bracketed. The process involves measuring the movement of the autocollimator beam relative to a reference associated with the segment as the carriage transits the granite beam in its normal acquisition mode. Typically, eight forward and backward passes are made and the data fitted with a 5^{th}-order polynomial. A typical example of the data acquired is shown in Figure 6.

The correction data, in the form of an array of slope angles, is then subtracted from the surface measurement data. Each bracket of the correction data is subtracted from the surface data separately to obtain an average base radius of curvature and conic constant. The actual difference in radius correction derived from each bracket is usually very small – well under 0.5 mm or about $6\text{x}10^{-4}$ % - and is much smaller than the errors derived from other sources.

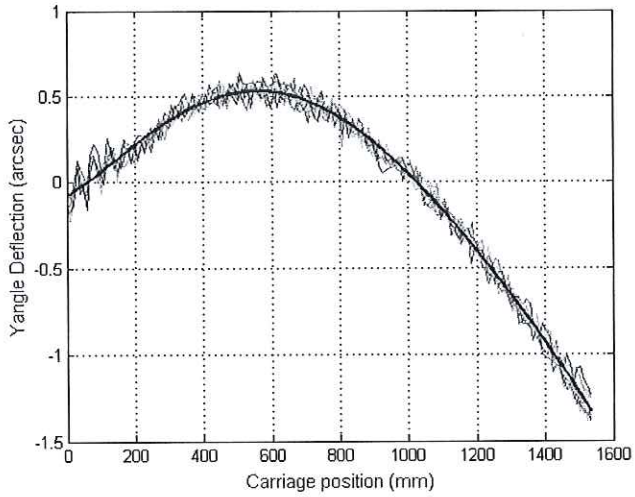

Figure 6. The deflection angle caused by the pitching of the autocollimator in response to the kinematic transit of the pentaprism carriage along the granite beam. The data was acquired over eight scans or iterations – four forward, four backward. Data from all eight iterations is shown with an averaged 5^{th}-order polynomial fit highlighted in bold. This fit is used to calculate the correction to subtract from the actual measurement data acquired at a different time.

5.3 Derivation of an absolute error

An estimate of the absolute error in the radius of curvature, R, can be determined by the following geometrical considerations. If x represents the scan as defined by the carriage movement over a typical scan length and θ is the angle subtended by x at the center of curvature, then typical values are $x \cong 1.1$ m and $R \cong 84$ m so that $R \gg x$ and hence

$$R \cong \frac{x}{\theta}. \tag{2}$$

Using propagation of errors theory, the uncertainty in R, ΔR, can be expressed as:

$$\Delta R = R\sqrt{\left(\frac{\Delta x}{x}\right)^2 + \left(\frac{\Delta \theta}{\theta}\right)^2}, \tag{3}$$

where the prefix " Δ" denotes the uncertainty in the given parameter, and an estimate of the absolute error in R can be determined. Typical uncertainty values are $\Delta\theta = 0.25$ arcsec ($1.212\text{x}10^{-6}$ rad), $\Delta x = 10$ microns ($10\text{x}10^{-6}$ m), $x = 1.1$ m and $\theta = 2456$ arcsec (1/84 rad), which give $\Delta R = 7.8$ mm using Equation 3. Varying the uncertainty values reveals that ΔR is dominated by the autocollimator uncertainty, therefore care has to be taken to maintain calibration of the autocollimator and optimize its performance by examining possible sources of deviation, such as temperature variation or relative mechanical movement.

6. MEASUREMENT POST-PROCESSING

The data from the NOM control software consists of encoder positions and orthogonal autocollimator slope angles at discrete points along the chosen scanlines as shown in Figure 4 and described in Section 4. The post-processing software allows corrections to be applied to the raw data as described in Section 5.2 and the slope angles are integrated with respect to encoder position to give the relative height profile within each scan. Note that the height profiles are not absolute and the relative heights and slopes of the different scans are unknown.

Each scan profile may then be analyzed separately using curve-fitting software or a number of scan profiles may be assembled together and analyzed using surface fitting software. Our post-processing software has been developed using MATLAB[5] and includes (i) circle curve fitting which is based on algorithms described in Chernov[6] and calculates the radius and center coordinates of the best fit circle, and (ii) conic surface fitting which uses non-linear least-squares optimization to obtain the best fit to the conic form as given in Equation 1.

The conic fitting software can assemble separate scans and allocates up to six degrees of freedom, three translations and three rotations, to each scan. Alternatively the scans along each scanline may be grouped together and six degrees of freedom allocated to each group. The optimization parameters consist of the base radius of curvature R_B and the conic constant k together with the chosen geometrical degrees of freedom.

The scans or scan groups are assembled to produce a first approximation to the surface using the initial values chosen for the optimization parameters. The geometrical transformation between the local NOM and the global M1 coordinate systems is used in the objective function to calculate the residual. A trust-region-reflective optimization technique is used to obtain the best surface fit which provides the optimized values of R_B and k and the geometrical degrees of freedom. In practice it is found that the piston and tilt of each scan are the most significant degrees of freedom and the iterative optimization converges quickly and gives consistent results essentially independent of the starting parameter values.

The circle fit and conic fit software algorithms are different and independent of each other. As an indication of consistency, data for the 1.45 m reference sphere was analyzed by the conic fitting software and was seen to give a conic constant of zero and a radius of curvature that agrees with the circle fits to the separate scans. Also circle fits to the different individual azimuthal scans of aspheric segments (see Figure 7) give radii of curvature that are consistent with the optimized surface given by the conic fitting software and agree with theoretical geometric calculations of the surface azimuthal curvature.

7. SAMPLE RESULTS

7.1 Data from one sample segment

Typical results are illustrated in Figure 7 which shows the profile of radii produced from circle-fitting the sagitta data derived from each of the ten scanlines (each scanned with forward and backward iterations) from a segment with the scanlines distributed as shown in Figure 4. Both corrected (using the back bracket correction data) and uncorrected data are shown. The correction compensates for the kinetic deflection of the autocollimator during measurement, and is described in Section 5.2.

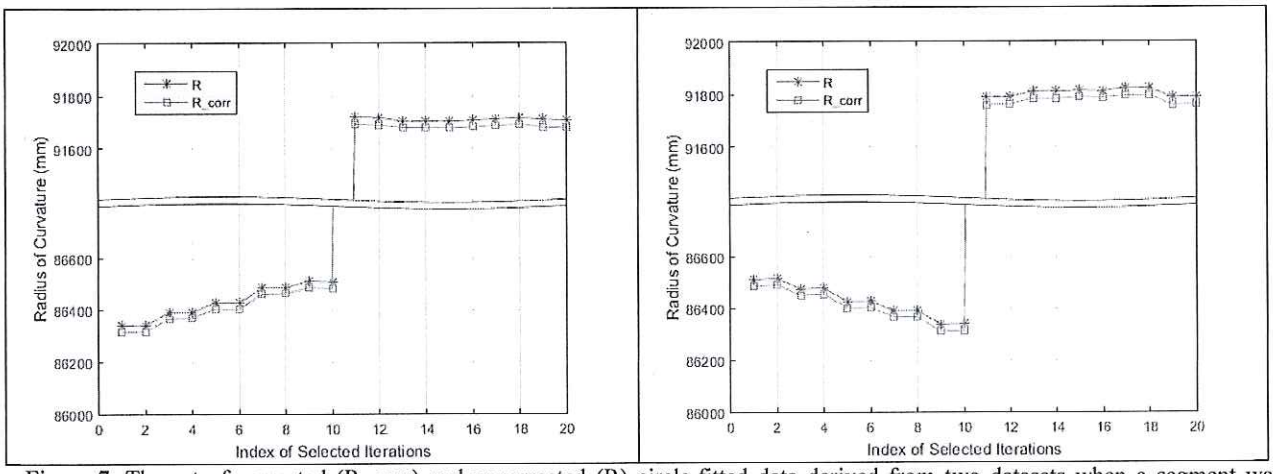

Figure 7. The set of corrected (R_corr) and uncorrected (R) circle-fitted data derived from two datasets when a segment was measured. The left plot reveals data from the 0 and 90 degrees orientations dataset, while the right plot displays the 180 and 270 degrees orientations dataset. Each dataset consists of 2 x 5 scanlines (2 x 10 iterations) as shown in Figure 4.

The left-hand plot in Figure 7 contains a dataset derived from all the ten scanlines or twenty scans in two orientations (0 and 90 degrees), while the right-hand plot does similarly with data from the other two orientations (180 and 270 degrees). For 0 and 180 degrees the radii increase or decrease, respectively, with a change of scanline, whereas, for 90 and 270 they essentially remain constant. For 0 and 180 degrees, the scanline arrays occupy different distances from the center of M1, therefore the radii of curvature measured tangential to the azimuthal lines should change with the scanline accessed. In contrast, at 90 and 270 degrees, the scanlines occupy approximately different radial lines of M1 and are essentially at the same distance from its center, so the radii measured should not vary systematically.

Using the conic fitting software to analyze the above data gives the results shown in Table 1. Four datasets were assimilated over two non-consecutive days – two datasets each day.

Table 1. Table of fitted R_B and conic constant (k) values for all datasets measured on a sample segment and derived using both front- and back-bracketed deflection error compensation data. A dataset is composed of two sets of five scanlines each containing a forward and a backward scan or iteration. The two sets are directed orthogonal to each other. The front-bracket refers to the deflection error data of the autocollimator as measured prior to surface measurements and the back-bracket to similar acquired subsequently.

Dataset	R_B (mm) derived using the front bracket	R_B (mm) derived using the back bracket
1	83859.84	83859.73
2	83858.42	83858.32
3	83856.36	83856.23
4	83855.37	83855.24
Average	**83857.50**	**83857.38**
Standard deviation	**2.01**	**2.03**
Dataset	**Conic Constant derived using the front bracket**	**Conic Constant derived using the back bracket**
1	-0.9938229	-0.9938231
2	-0.9938439	-0.9938441
3	-0.9947851	-0.9947879
4	0.9940692	0.9940720
Average	**-0.99413**	**-0.99413**
Standard deviation	**0.00045**	**0.00045**

7.2 Measurement error analysis

The specification demands that we have knowledge of R_B of all the segments to within ±14 mm and that the first segment produced and measured is within ± 200 mm of 84000 mm.

If the figures from Table 1 are appropriately averaged and an uncertainty based on standard deviation is estimated, the calculated parameter values are

$$R_B = 83857.44 \pm 1.87 \text{ mm} \qquad \text{and} \qquad k = -0.99413 \pm 0.00042,$$

which indicates that the measurement uncertainty in R_B, is within the 2 to 3 mm target

The deflection correction has a significant effect on the results; if the deflection correction is not applied to dataset 1 in Table 1, the R_B calculated is 83882.28 mm with k = -0.9947114.

To further support data consistency, repeatability measurements are also included within the measurement campaign. These involve multiple scans across the central scanline when the segment is oriented at 0 degrees. Usually two sets of ten to twenty iterations are measured with a segment actuation between, where the actuators supporting the segment, see Figure 1, are lowered then raised back to the measuring height, which corresponds to the level used for interferometry.

Figure 8 shows the results from two repeatability sets applied to a segment, and are typical when air circulation and temperature are well-controlled. The uncertainty in the local azimuthal radius of curvature, as expressed through the standard deviation, ranges from about 0.8 mm before and 1.1 mm after actuation. This spread of results is well within the required specification of 2 to 3 mm mentioned earlier.

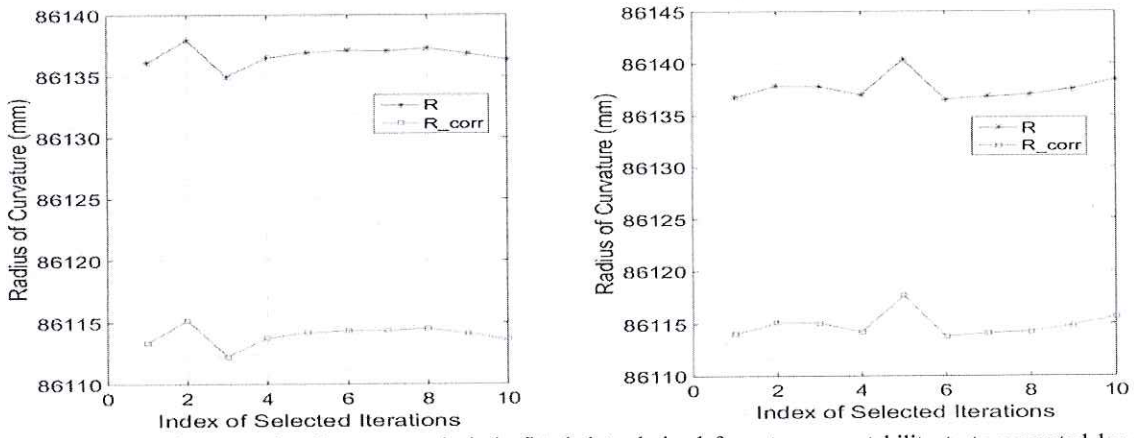

Figure 8. The set of corrected and uncorrected circle fitted data derived from two repeatability tests separated by a segment actuation, see text. At left are the measurements derived prior to the actuation with summary statistics for corrected data - mean: 86113.97 mm; standard deviation: 0.796 mm; range: 2.99 mm. At right are the measurements derived subsequent to the actuation with summary statistics - mean: 86114.87 mm; standard deviation: 1.14 mm; range: 3.83 mm.

For the base radius of curvature, uncertainties of approximately ± 2 mm have been found typical in the measurement campaigns The uncertainty associated with the radius quoted above is the measurement error, however, the absolute error estimated earlier (about 8mm) must be combined with it to obtain the overall error – about ± 8.5 mm, typically. At the time of writing, 4 segments have been polished and measured. The average R_B is 83853.7 mm, with a standard deviation of 5.4 mm, and therefore satisfies the constraints set out in Section 2.

8. CONCLUSIONS

Previous NOM systems have been used for measuring near-flat X-ray optics in closely controlled laboratory environments and have utilized a narrow range of autocollimator angles. The development of the Glyndŵr NOM demonstrates that the NOM concept can be used successfully in an industrial fabrication environment to measure curved spherical and aspheric surfaces. We use the autocollimator to its full angular dynamic range and over a wide range of operating distances.

We have developed procedural and numerical methods to derive fitted conic surfaces from NOM data to a high degree of accuracy and repeatability. Although the angular range of current autocollimators can restrict scan lengths for more highly curved surfaces, the Glyndŵr University system has the required accuracy of 1 part in 10,000 for the segment optics described in this paper. A significant effort was required to detect and correct for optomechanical effects which were found to be extremely important and had to be determined to a high degree of accuracy in order to characterize the system correctly.

Current activity at Glyndŵr is concerned with improved methods for the optical calibration of the autocollimator over its full dynamic ranges of angle and operating distance. To reduce deployment time, we are investigating methods to simultaneous measure the optomechanical deflection and surface data. Also work to date has concentrated on measuring optics having large radii of curvature which are difficult to determine using other techniques and future work will also consider the utility of the method for shorter radius optics and other applications.

ACKNOWLEDGEMENTS

The authors wish to thank the following organizations for loan of equipment and technical assistance: Spectrum Metrology Ltd. and Armstrong Optical Ltd.

REFERENCES

[1] Alcock, S., Sawhney, K., Scott, S., Pedersen, U., Walton, R., Siewert, F., Zeschke, T., Senf, F., Noll, T., and Lammert, H., "The Diamond-NOM: A non-contact profiler capable of characterizing optical figure error with sub-nanometer repeatability," Nuclear Instruments and Methods in Physics Research Section A: Accelerators, Spectrometers, Detectors and Associated Equipment 616(2-3), 224-228 (2010).

[2] Siewert, F., Noll, T., Schlegel, T., Zeschke, T., and Lammert, H., "The nanometer optical component measuring machine: a new sub-nm topography measuring device for x-ray optics at BESSY," AIP Conference Proceedings 705(1), 847-850 (2004).

[3] Siewert, F., Lammert, H., and Zeschke, T., "The Nanometer Optical Component Measuring Machine," Modern Developments in X-Ray and Neutron Optics, Springer, Berlin (2008).

[4] Atkins, C., Mitchell, J., and Rees, P. C. T., "Non-contact profilometry of E-ELT segments at OpTIC Glyndŵr," Proc. SPIE, 8126(21), (2011).

[5] MATLAB Release 2015a, The MathWorks, Inc., Natick, Massachusetts, United States.

[6] Chernov, N., [Circular and Linear Regression: Fitting Circles and Lines by Least Squares], Chapman & Hall/CRC Monographs on Statistics & Applied Probability, ISBN-10: 143983590X, ISBN-13: 978-1439835906 (2010).